ACES Asian Chemical Editorial Society

DOI: 10.1002/ajoc.201900085

ASIAN JOURNAL OF ORGANIC CHEMISTRY Communication

Synthesis of Redox-switchable 5,15-Dialkyl-10,20-diaryl-5,15-diazaporphyrins and Diversification of their *N*-Alkyl Groups

Mai Mutoh,[a] Keisuke Sudoh,[b] Ko Furukawa,[c] Mao Minoura,[d] Haruyuki Nakano,[e] and Yoshihiro Matano*[a]

Abstract: Nickel(II) and copper(II) complexes of redox-switchable 20π, 19π, and 18π 5,15-dialkyl-10,20-diaryl-5,15-diazaporphyrins were prepared through a metal-templated cyclization method. Furthermore, the terminal silyloxy groups in the peripheral *N*-alkyl chains were transformed into hydroxy groups by deprotection. It is worth noting that redox reactions between the 19π and 18π systems bearing hydroxy groups caused a change in the water solubility of the diazaporphyrin chromophore.

Porphyrins are known as redox-switchable photosensitizers with large absorption coefficients in the visible region and have been applied in many fields such as photovoltaics, sensors, light-emitting diodes, etc.[1] However, reduced forms of porphyrins (19π and 20π porphyrins) are extremely air-sensitive, and this property has made it difficult to extensively study the correlation between the redox processes and optical/magnetic properties.[2–13] Recently, we proposed a new approach, replacement of *meso*-methine units with nitrene (RN) units, to provide air-stability to reduced forms of a porphyrin ring, and reported the first examples of redox-switchable 20π, 19π, and 18π 5,10,15,20-tetraaryl-5,15-diazaporphyrinoids (5,15-Ar_2DAPs), **P0**, **P1**, and **P2** (Scheme 1),[14] and related compounds.[15,16] As the unshared electron pairs in the p orbitals of two *meso*-nitrogen atoms can be used for resonance, the reduced forms **P0** and **P1** (neutral 20π and cationic 19π derivatives) are considerably stabilized compared with those of isoelectronic porphyrin counterparts (dianionic 20π and anionic 19π derivatives, respectively). Furthermore, 5,15-Ar_2DAPs undergo stepwise redox reactions between 18π and 20π oxidation states, and can reversibly change their color. From a structural point of view, **P2** is recognized as a hybrid of diazaporphyrin and *N,N'*-diarylviologen. It is known that *N*-substituents of viologen directly affect the redox and physiological properties as well as the solubility of the entire molecule.[17] This means that modification of the *N*-substituents is a reliable strategy for the development of viologen-based electrochromic materials. With this in mind, we designed a new hybrid dye, 5,15-dialkyl-10,20-diaryl-5,15-diazaporphyrin (5,15-R_2DAPs; R = alkyl groups) having hydrophobic or hydrophilic alkyl chains on the *meso*-nitrogen atoms of the diazaporphyrin chromophore.

Herein, we report the first synthesis of nickel(II) and copper(II) complexes of 5,15-R_2DAP using metal-templated cyclization and redox reactions. The color of 5,15-R_2DAP varied widely depending on the oxidation states, while the hydrophilicity was controlled by diversification of the *N*-alkyl groups.

Initially, we prepared nickel(II) and copper(II) complexes of 5,15-R_2DAP (Scheme 2). Treatment of nickel(II) acetate with 1-(butylamino)-9-chloro-5-mesityldipyrrin **1a** (mesityl = 2,4,6-trimethylphenyl) in the presence of triethylamine at room temperature afforded the nickel(II)–bis(dipyrrin) complex **2a**. Heating a mixture of **2a** and sodium *tert*-butoxide (NaO*t*-Bu) in refluxing toluene gave the nickel(II) complex of 20π 5,15-

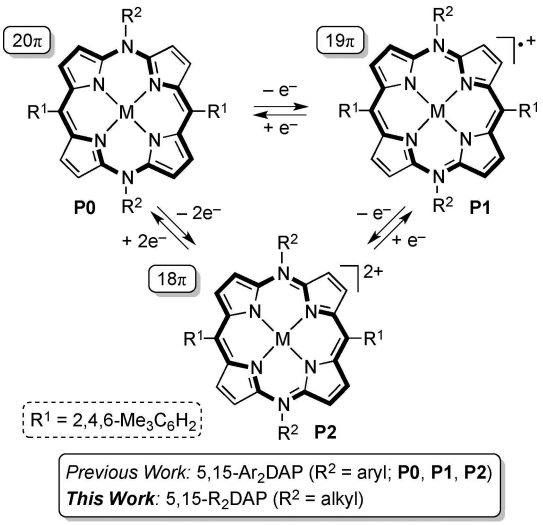

Scheme 1. Redox reactions of *meso*-*N*-substituted 5,15-diazaporphyrins.

[a] *M. Mutoh, Prof. Dr. Y. Matano*
Department of Chemistry, Faculty of Science,
Niigata University, Nishi-ku, Niigata 950-2181 (Japan)
E-mail: matano@chem.sc.niigata-u.ac.jp

[b] *K. Sudoh*
Department of Fundamental Sciences, Graduate School of Science and Technology
Niigata University, Nishi-ku, Niigata 950-2181 (Japan)

[c] *Prof. Dr. K. Furukawa*
Center for Coordination of Research Facilities, Institute for Research Promotion
Niigata University, Nishi-ku, Niigata 950-2181 (Japan)

[d] *Prof. Dr. M. Minoura*
Department of Chemistry, College of Science,
Rikkyo University, Toshima-ku, Tokyo 171-8501 (Japan)

[e] *Prof. Dr. H. Nakano*
Department of Chemistry, Graduate School of Science,
Kyushu University, Nishi-ku, Fukuoka 819-0395 (Japan)

Supporting information for this article is available on the WWW under https://doi.org/10.1002/ajoc.201900085

Bu_2DAP **3Ni-a** as a sole product. Oxidation of **3Ni-a** with silver(I) hexafluorophosphate ($AgPF_6$) in CH_2Cl_2 quantitatively produced the 19π radical cation **4Ni-a** or 18π dication **5Ni-a**, depending on the amount of the oxidant used. Alternatively, **4Ni-a** could be prepared by the comproportionation reaction between equimolar amounts of **3Ni-a** and **5Ni-a**. It is noteworthy that the 19π radical cation **4Ni-a** was isolated as an air-stable solid and did not decompose at all during chromatographic separation on a silica-gel column. The other two 5,15-R_2DAPs, **3Ni-a** and **5Ni-a**, were isolated by recrystallization. Similarly, the nickel (II) complexes of 5,15-$(TBSOCH_2CH_2CH_2)_2$DAP (TBS = *tert*-butyldimethylsilyl) **3Ni-b** and **4Ni-b** were prepared from nickel (II)-bis(dipyrrin) complex **2 b**, which was readily available from **1 b**. When **1 a** was treated with an equimolar amount of copper (II) acetate, the 19π radical cation **4Cu-a** was obtained quantitatively after exchange of the counter anion. It is probable that an initially formed copper(II)-bis(dipyrrin) complex readily underwent the copper-promoted cyclization-oxidation reactions to directly afford the 19π derivative, as previously reported for the preparation of **P1** (M = Cu). This type of one-pot synthesis was also effective for obtaining **4Cu-b** from **1 b**.

The newly prepared 5,15-R_2DAPs were characterized by high-resolution electrospray ionization (ESI) mass spectrometry and ^{1}H NMR spectroscopy. The ^{1}H NMR spectra of **3Ni-a,b** in C_6D_6 showed their β-pyrrolic and *N*-CH_2 protons in the relatively upfield region (δ = 4.15–5.19 and 1.89–2.21 ppm, respectively), which reflected the paratropic ring-current in their porphyrin rings (Figures 1a and S1 in the Supporting Information, SI); the 20π-electron circuits of **3Ni-a,b** were anti-aromatic in character. The shielding effects observed for the β-pyrrolic protons of **3Ni-a,b** were rather small compared with those observed for **P1** (M = Ni, R^2 = *p*-$MeOC_6H_4$), in which the peripheral protons at the 3,7,13,17 positions experienced additional shielding derived from the diatropic ring-current in the neighboring aryl rings at the 5 and 15 positions. By contrast, **5Ni-a** showed the ^{1}H NMR peaks that reflected the diatropic ring-current in the porphyrin ring (Figure S10 in the SI); the 18π-electron circuit of **5Ni-a** was aromatic in character. Electron paramagnetic resonance (EPR) spectroscopy of **4Ni-a** showed a signal at g = 1.9927 with hyperfine structures (Figure 1b). The experimentally determined hyperfine coupling constants (A_X; X = ^{14}N, ^{1}H) reflected high spin densities at the two *meso*-nitrogen and four β-pyrrolic hydrogen atoms, as predicted by density functional theory (DFT) calculation on the 19π model compound, **4Ni-m** (in Scheme 1, without PF_6^-).

The crystal structure of **4Ni-a** was unambiguously elucidated by X-ray diffraction analysis at the SPring-8 synchrotron facilities. As shown in Figure 2 and Figure S2 in the SI, **4Ni-a** had a ruffled DAP π-plane with a root-mean-square deviation (Δd_{RMS}) of 0.225 Å, which was considerably larger than the Δd_{RMS} value of **P1** (M = Ni, R^2 = *p*-*t*-BuC_6H_4; 0.044 Å). This probably arose from the steric repulsion between the β-pyrrolic hydrogen atoms and *N*-CH_2 groups. The structural feature of **4Ni-a** resembled that of 19π model **4Ni-m**. The relatively short C1/C2–N2 and C4/C5–N5 bond lengths (average value = 1.358 Å) indicated that the unshared electron pairs in the p orbitals of the *meso*-N atoms were conjugated with the π-orbitals in the adjacent α-pyrrolic carbon atoms. The average Ni–N bond length of pseudo square planar **4Ni-a** (1.918 Å) was appreciably longer than that of octahedral **P1** (M = Ni, R^2 = *t*-BuC_6H_4; 1.986 Å), which should reflect their different coordination environments.

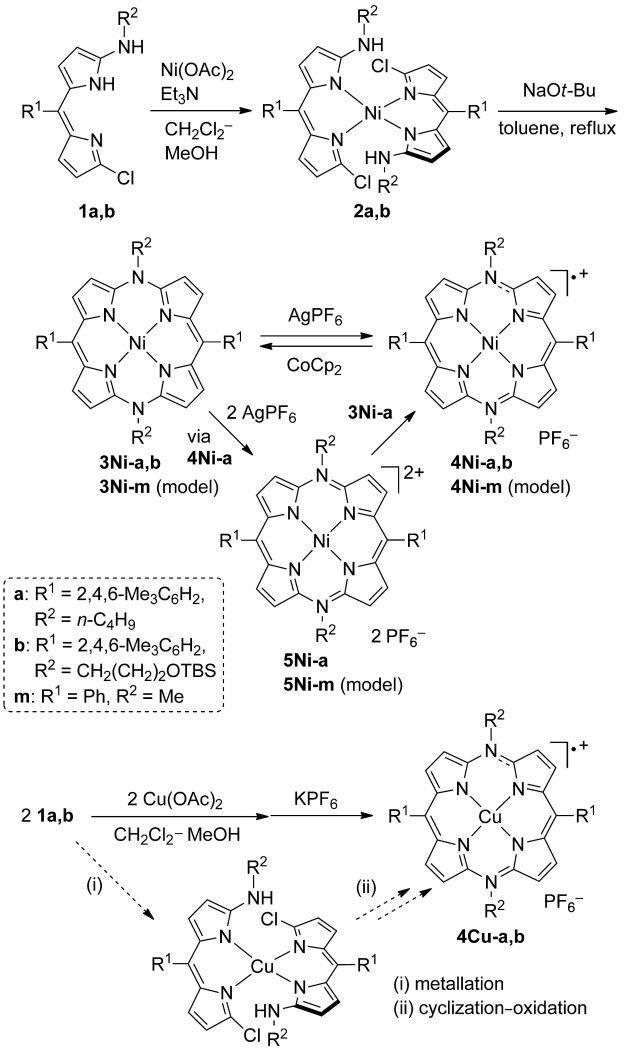

Scheme 2. Synthesis of nickel(II) and copper(II) complexes of 5,15-dialkyl-10,20-dimesityl-5,15-diazaporphyrins.

The redox potentials of **4Ni-a** and **4Cu-a** in CH_2Cl_2 were measured by using cyclic voltammetry with Bu_4NPF_6 as a supporting electrolyte (Table 1). As shown in Figure 3a, **4Ni-a** exhibited two reversible redox processes at $E_{1/2}$ = −0.60 and +0.07 V vs. ferrocene/ferrocenium (Fc/Fc^+), which were attributed to 20π/19π and 19π/18π redox reactions, respectively. The half-wave potentials of 5,15-Bu_2DAP were slightly shifted to the positive side compared with those of 5,15-Ar_2DAP **P1** (M = Ni, R^2 = Ph; $E_{1/2}$ = −0.59 and +0.10 V vs. Fc/Fc^+), which suggested that replacing the *N*-substituents from phenyl to *n*-butyl groups slightly changed the energy levels of the highest occupied molecular orbital (HOMO) and lowest unoccupied molecular orbital (LUMO) of the diazaporphyrin ring. The experimentally observed results were basically supported by the theoretically

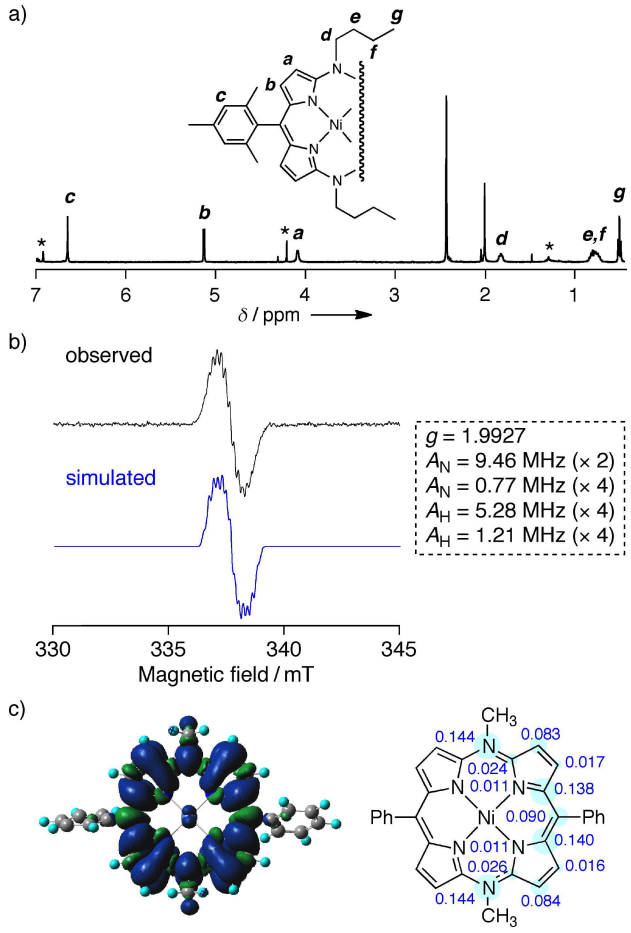

Figure 1. a) ^{1}H NMR spectrum (δ 7.0–0.5 ppm) of **3Ni-a** in C_6D_6. Asterisks indicate the residual solvents. b) EPR spectra of **4Ni-a**: observed in CH_2Cl_2 at 298 K (upper) and simulated (lower). c) Spin density distribution at the optimized structure (upper) and spin densities at the DAP ring (lower) of **4Ni-m**; calculated by the DFT method with the solvent effect (PCM, CH_2Cl_2).

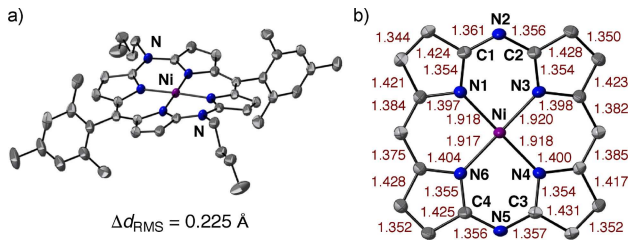

Figure 2. a) ORTEP diagram (50% probability ellipsoids) of **4Ni-a** (CCDC-1886906). Hydrogen atoms, counter PF_6^- ion, and solvent molecules are omitted for clarity. Δd_{RMS} = root mean square deviation of the 24 C/N atoms from the mean diazaporphyrin π-plane. b) Bond lengths (Å) except the standard deviations (0.002–0.005 Å) are shown in red.

calculated results for their models, **3Ni-m** and **5Ni-m** (Figure S3 in the SI); the HOMO of **3Ni-m** (E = −4.44 eV) and the LUMO of **5Ni-m** (E = −5.21 eV) were stabilized compared with the corresponding orbitals of **P0-m** (E = −4.26 eV) and **P2-m** (E = −5.16 eV), respectively, (M = Ni, $R^1 = R^2$ = Ph) at the same level of theory. The relatively large stabilization of the HOMO level of **3Ni-m** may reflect its significantly distorted diazaporphyrin ring

Table 1. Optical and redox properties of 5,15-R_2DAP.[a]

Compd	λ_{max} (log ε)	$E_{1/2}$[b]
3Ni-a	443 (4.78), 542 (4.73)	–
3Ni-b	442 (4.82), 541 (4.76)	–
4Ni-a	316 (4.55), 386 (4.60), 445 (4.72), 866 (4.33)	−0.60, +0.07
4Ni-b	318 (4.48), 386 (4.63), 444 (4.75), 866 (4.34)	−0.62, +0.07
5Ni-a	339, 395, 636 [c]	–
4Cu-a	321 (4.46), 387 (4.66), 443 (4.73), 868 (4.43)	−0.63, +0.06
4Cu-b	319 (4.46), 388 (4.70), 443 (4.79), 869 (4.50)	−0.63, +0.06
6Cu	318 (4.48), 388 (4.70), 443 (4.79), 869 (4.51)	−0.63, +0.04
7Cu	344 (4.33), 393 (4.71), 635 (4.68) [d]	–

[a] Measured in CH_2Cl_2 unless otherwise noted. [b] Half-wave potentials for 20π/19π and 19π/18π processes vs. ferrocene/ferrocenium couple (with Bu_4NPF_6). [c] Extinction coefficients were not determined. [d] λ_{max} = 384, 630 nm in H_2O.

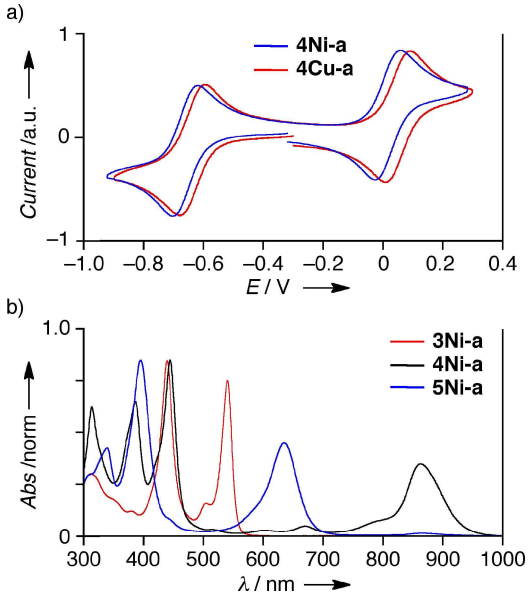

Figure 3. a) Cyclic voltammograms of **4Ni-a** and **4Cu-a** in CH_2Cl_2 with Bu_4NPF_6: E vs. ferrocene/ferrocenium. b) Normalized UV/Vis/NIR absorption spectra of **3Ni-a**, **4Ni-a**, and **5Ni-a** in CH_2Cl_2.

at the optimized structure; the *meso*-N and *meso*-C atoms deviated from the mean π-plane by 0.62–0.81 Å. Changing the central metal from Ni to Cu did not significantly impact the redox potentials. The $E_{1/2}$ values of **4Ni-b** and **4Cu-b** were almost the same as those of **4Ni-a** and **4Cu-a**, respectively (Figure S4 in the SI).

The optical properties of 5,15-R_2DAP in CH_2Cl_2 were investigated by ultraviolet-visible-near infrared (UV/vis/NIR) absorption spectroscopy (Table 1 and Figures 3b and S5 in the SI). As shown in Figure 3b, **3Ni-a**, **4Ni-a**, and **5Ni-a** exhibited intense absorption bands with different absorption maxima (λ_{max}), which were close to the values reported for the corresponding counterparts, **P0**, **P1**, and **P2**, respectively. The lower-energy bands of **3Ni-a** (λ_{max} = 542 nm), **4Ni-a** (λ_{max} = 866 nm), and **5Ni-a** (λ_{max} = 636 nm) were assigned to the HOMO-to-LUMO + 1, HOMO − 1-to-SOMO, and HOMO-to-LUMO electronic transitions, respectively, based on the results of the time-dependent DFT calculations (Table S3 in the SI). The

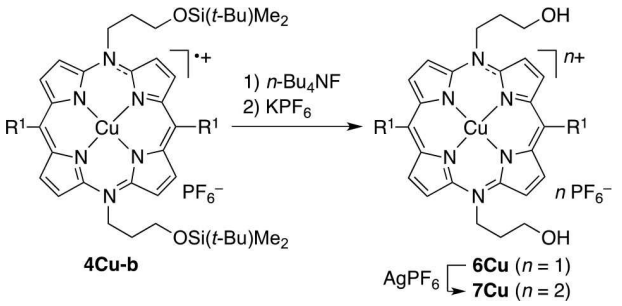

Scheme 3. Synthesis of **6Cu** and **7Cu**.

longest absorption maximum of **5Ni-a** was significantly red-shifted compared with that of nickel(II) complex of 10,20-dimesityl-5,15-diazaporphyrin,[18] which indicated that introducing a viologen-like structure improved the light-harvesting ability of the diazaporphyrin chromophore in the long-wavelength visible region. The copper(II) complexes also showed the characteristic absorption spectra (Figures S5b,c in the SI). The terminal functional groups of the *N*-alky chains had negligible effects on the λ_{max} values.

Finally, we conducted deprotection of the *O*-silyl groups in the *N*-alkyl chains of **4Cu-b** by treatment with Bu_4NF, which afforded 19π 5,15-bis(3-hydroxypropyl)DAP **6Cu** (Scheme 3). Furthermore, oxidation of **6Cu** with $AgPF_6$ afforded the 18π dication **7Cu**. Although **6Cu** did not dissolve in water, **7Cu** was slightly soluble in water. This indicated that the increase in the charge from +1 to +2 improved the hydrophilic character of the diazaporphyrin chromophore. The absorption maximum of **7Cu** in H_2O was blue-shifted compared with that in CH_2Cl_2, and adding excess chloride ion increased its absorbance (Figure S5d in the SI). These results implied that the counter anion also played an important role in producing the water solubility.

In summary, we have established a convenient method for the synthesis of metal(II) complexes of 5,15-dialkyl-10,20-diaryl-5,15-diazaporphyrin, which have primary alkyl groups on the two *meso*-*N* atoms. The 20π, 19π, and 18π oxidation states were generated reversibly by chemical and electrochemical redox reactions. Remarkably, the 19π radical cations were extremely stable in air and on a silica-gel column. Furthermore, chemical modification of the *N*-alkyl groups significantly changed the hydrophilic character of the entire diazaporphyrin chromophore. The present study provides valuable information regarding the construction of viologen-like diazaporphyrins with remarkable electrochromic behavior in a wide range of the UV/vis/NIR region and with water solubility. The primary hydroxy groups incorporated in the *N*-alkyl chains could be converted to various functional groups, which were, therefore, useful for the development of diazaporphyrin-containing materials. Further studies on the interdisciplinary area of porphyrin and viologen are now in progress.

Acknowledgements

This work was supported by JSPS KAKENHI (Grant Number: 18H01961 to YM, 15K05392 and 18K05036 to HN). We would like to express our gratitude to the SPring-8 synchrotron, where synchrotron radiation experiments were performed at the BL40XU beamline with the approval of the Japan Synchrotron Radiation Research Institute (JASRI) (proposals 2018A1405 and 2018B1275).

Conflict of Interest

The authors declare no conflict of interest.

Keywords: porphyrinoids · diazaporphyrin · dyes/pigments · template synthesis · macrocyclic ligands

[1] For example, see: a) L.-L. Li, E. W.-G. Diau, *Chem. Soc. Rev.* **2013**, *42*, 291–304; b) Y. Ding, W.-H. Zhu, Y. Xie, *Chem. Rev.* **2017**, *117*, 2203–2256; c) Y. Ding, Y. Tang, W. Zhu, Y. Xie, *Chem. Soc. Rev.* **2015**, *44*, 1101–1112.
[2] G. L. Closs, L. E. Closs, *J. Am. Chem. Soc.* **1963**, *85*, 818–819.
[3] J. W. Buchler, L. Puppe, *Liebigs Ann. Chem.* **1970**, *740*, 142–163.
[4] G. N. Sinyakov, A. M. Shul'ga, I. V. Filatov, G. P. Gurinovich, *Theor. Exp. Chem.* **1988**, *24*, 37–44.
[5] R. Cosmo, C. Kautz, K. Meerholz, J. Heinze, K. Müllen, *Angew. Chem. Int. Ed. Engl.* **1989**, *28*, 604–607; *Angew. Chem.* **1989**, *101*, 638–640; *Angew. Chem. Int. Ed.* **1989**, *28*, 604–607
[6] K. M. Kadish, E. Van Caemelbecke, G. Royal, in *The Porphyrin Handbook Vol 8* (Eds.: K. M. Kadish, K. M. Smith, R. Guilard), Academic Press, San Diego, **2000**, pp 1–114.
[7] T. Yoshida, W. Zhou, T. Furuyama, D. B. Leznoff, N. Kobayashi, *J. Am. Chem. Soc.* **2015**, *137*, 9258–9261.
[8] K. Reddy, A. Basavarajappa, M. D. Ambhore, V. G. Anand, *Chem. Rev.* **2017**, *117*, 3420–3443.
[9] M. Horie, Y. Hayashi, S. Yamaguchi, H. Shinokubo, *Chem. Eur. J.* **2012**, *18*, 5919–5923.
[10] T. Sugai, M. Minoura, H. Nakano, Y. Matano, *Bull. Chem. Soc. Jpn.* **2018**, *91*, 1264–1266.
[11] W. Suzuki, H. Kotani, T. Ishizuka, Y. Shiota, K. Yoshizawa, T. Kojima, *Angew. Chem. Int. Ed.* **2018**, *57*, 1973–1977; *Angew. Chem.* **2018**, *130*, 1991–1995.
[12] Y. Matano, *Chem. Rev.* **2017**, *117*, 3138–3191.
[13] D. Shimizu, A. Osuka, *Chem. Sci.* **2018**, *9*, 1408–1423.
[14] a) T. Satoh, M. Minoura, H. Nakano, K. Furukawa, Y. Matano, *Angew. Chem. Int. Ed.* **2016**, *55*, 2235–2238; *Angew. Chem.* **2016**, *128*, 2275–2278; b) K. Sudoh, T. Satoh, T. Amaya, K. Furukawa, M. Minoura, H. Nakano, Y. Matano, *Chem. Eur. J.* **2017**, *23*, 16364–16373.
[15] K. Sudoh, T. Hatakeyama, K. Furukawa, H. Nakano, Y. Matano, *J. Porphyrins Phthalocyanines* **2018**, *22*, 542–551.
[16] Y. Matano, T. Shibano, H. Nakano, Y. Kimura, H. Imahori, *Inorg. Chem.* **2012**, *51*, 12879–12890.
[17] a) C. L. Bird, A. T. Kuhn, *Chem. Soc. Rev.* **1981**, *10*, 49–82; b) P. M. S. Monk, *The Viologens: Physicochemical Properties, Synthesis and Applications of the Salts of 4,4'-Bipyridine*, Wiley, Chichester, **1998**; c) R. J. Mortimer, *Electrochimica Acta*, **1999**, *44*, 2971–2981; d) R. J. Mortimer, D. R. Rosseinsky, P. M. S. Monk, *Electrochromic Materials and Devices*, Wiley-VCH, Weinheim, **2015**; e) L. Striepe, T. Baumgartner, *Chem. Eur. J.* **2017**, *23*, 16924–16940.
[18] Y. Matano, T. Shibano, H. Nakano, H. Imahori, *Chem. Eur. J.* **2012**, *18*, 6208–6216.

Manuscript received: February 6, 2019
Accepted manuscript online: February 8, 2019
Version of record online: February 20, 2019